



Oblique Incidence Sound Absorption of Parallel Arrangement of Thin Microperforated Panel (MPP)

Iwan Prasetyo¹, Indra Sihar^{1,2}, Anugrah Sabdono Sudarsono¹

¹Engineering Physics, Faculty of Industrial Technology, Institut Teknologi Bandung, Ganesa Street 10 Bandung 40132, Indonesia.

i.prasetyo@fti.itb.ac.id, anugrah@tf.itb.ac.id

²Department of Built Environment, Eindhoven University of Technology, PO Box 513, 5600 MB Eindhoven, The Netherlands.

i.sihar@tue.nl

Abstract

In this study, the absorption coefficient of a thin parallel MPP at oblique incidence angle is investigated. The thin structure is introduced by a coiling shape as a backing air cavity, and the parallel configuration is applied to have a wider sound absorption bandwidth than a single MPP. The effects of the oblique sound incidence on the thin parallel MPP are investigated by numerical studies. It is found that the oblique incidence can result in lower sound absorption and a shift in resonance absorption, especially for high incidence angles, e.g. $> 70^\circ$. In addition, the performance of the thin MPP at normal incidence angle can be maintained for the incident angle $< 60^\circ$. This observation is strongly depend on the overall width of the MPP surface. The ratio between the wavelength of the incident wave and the overall width dimensions of the MPP is critical. Depend on this ratio, the deterioration of the sound absorption can be observed and that is associated with breakdown frequency. Moreover, the use of two MPPs under parallel arrangement introduces complexity with respect to the wavelength of the oblique incidence. The presence of coiled cavity also introduces another factor determining the breakdown frequency rather than overall width dimensions solely. It is expected that current study can suggest ways to make the proposed structure insensitive to the change of incidence angle, which is important for dealing with the actual sound field in practice.

Keywords: Thin MPP absorber, coiled backing cavity, oblique incidence sound absorption

1 Introduction

It has been recognized that normal and oblique incidence can result in significantly different responses from sound absorbers [1, 2]. This scenario is less critical when dealing with isotropic fibrous porous materials. It is more obvious, however, for resonant sound absorbers, such as microperforated panel (MPP) absorbers that operate via Helmholtz resonator mechanism. Numerous investigations on parallel MPP with distinct air cavities are available in [3, 4]. While the dimensions of the unit parallel MPP important in normal incidence, the cavity features also affect the absorption behavior in the oblique case. In the oblique situation, matching impedance corrections can result in decreased absorption and a shift in the absorption resonance.

Coiled structures have been used to fabricate metamaterial structures capable of manipulating anomalous waves [5-9], and to realize subwavelength structures [10-12]. Additionally, thin parallel MPP can be produced by using a coiled structure to support the air cavity [13-15]. The required cavity length can be twisted in specific orientations, thereby lowering the total cavity thickness in the axial direction. This is advantageous because it results in a thinner MPP absorber, but the effect of normal and oblique incidence on the resulting absorption should be evaluated further. This is significant because the coiled structure

comprises an effective wave path proportional to the total cavity depth, which is absent from a straight air cavity. Thus, for similar targeted absorption qualities, it is important to investigate the implications of the coiled air cavity and to have a better understanding of the sound absorption behavior in relation to the incidence angle and MPP dimensions. Additionally, the study is expected to identify strategies to make the suggested structure insensitive to changes in the incident angle, which is critical for dealing with the actual sound field encountered in practice.

2 Methodology

In this section, a case study of the thin parallel MPP absorber is presented. This section presents a case study of the thin parallel MPP absorber. The absorption coefficient is calculated numerically for various incident angles. The numerical technique is the finite element method (FEM) via COMSOL Multiphysics 5.6, and the frequency range of interest is between 125 Hz and 2200 Hz.

2.1 Thin Parallel MPP structures

The MPP's coiled parallel structures are shown in Figure 1 (a). To keep things simple, the sub-MPPs all have the same perforations, with the widths of each sub-MPP being L_1 and L_2 , respectively. Therefore, the resonance frequencies of MPP-1 and MPP-2 are determined by the cavities D_1 and D_2 , where the air cavity of MPP-1 is coiled, as illustrated in Figure 1(b). By keeping L_1 and L_2 are smaller than D_1 and D_2 , the resonance absorption characteristics are determined only by the cavity depths and parallel absorption mechanisms. The unit cell is defined in this work as a system comprised of two parallel MPPs, as seen in Figure 1(c).

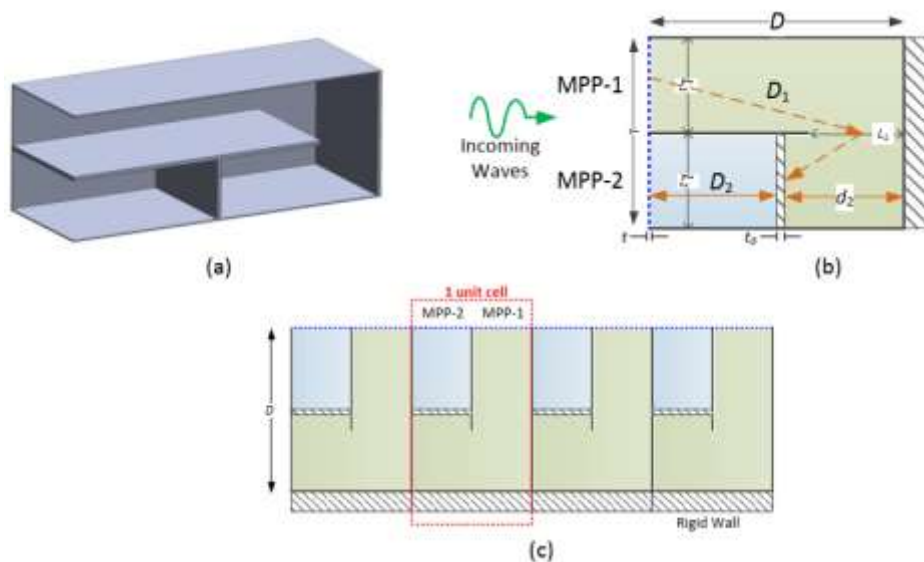


Figure 1- Thin parallel structure of MPP: (a) 3D-coiled structure, (b) schematic of coiled parallel MPP, and (c) definition of unit cell in a periodic arrangement

2.2 Finite Element Method (FEM)

The thin parallel MPP structure is modelled using FEM in the 2-D configuration depicted in Figure 1. The computational domain and the boundary conditions (BC) are shown in Figure 2.

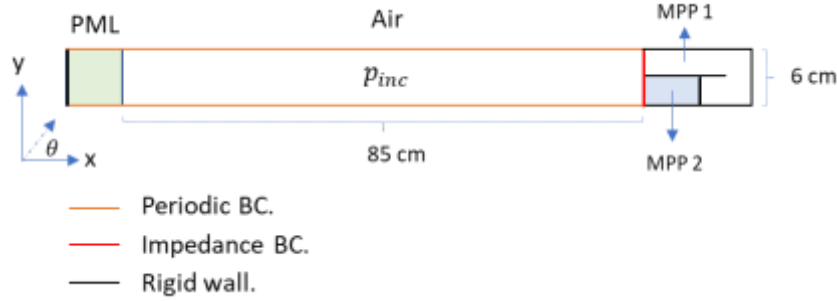


Figure 2. The coiled parallel MPP domain simulated using FEM.

In Figure 2, it is shown that $p_{inc} = \exp(-i(k_x x + k_y y))$ [Pa] is defined in the air region with the angle of incidence θ [°] as the incoming waves to the surface of the MPP. The $k_x = k \cos(\theta)$, and $k_y = k \sin(\theta)$, with $k = \omega/c_0$ as the wavenumber. c_0 is the sound speed in air, 345 [m/s]; $\omega = 2\pi f$ is the angular velocity with f as the sound frequency [Hz]. To allow the sound energy to propagate to the absorber, the incidence velocity vector is defined by Euler's method where $\mathbf{v}_{inc} = \nabla p_{inc} / i\omega\rho_0$ [m/s]. Structural vibration is omitted, where the MPP effect can be implemented as boundary condition impedance as

$$Z_{MPP-i} = r_i + jx_{mi}, \quad (1)$$

where r_i , and x_{mi} are the sub-MPP i , resistance and reactance, respectively. The resistance and the reactance are defined as follows [16]:

$$r = \frac{32\eta t}{\phi\rho_0 c d^2} \left(\left[1 + \frac{k^2}{32} \right]^{1/2} + \frac{\sqrt{2}}{32} k \frac{d}{t} \right)$$

$$x_m = \frac{\omega t}{\phi c} \left(1 + \left[1 + \frac{k^2}{2} \right]^{-1/2} + 0.85 \frac{d}{t} \right).$$

The $k = d\sqrt{\omega\rho_0/4\eta}$, with d is the pore diameter, ω is the angular frequency, ρ_0 is the air density, η is the dynamic viscosity of air, t is the panel thickness, and ϕ is the perforation ratio.

The geometry details on the MPP 1 and MPP 2 are shown in Figure 1, where the value of t is assumed negligible. The Perfectly Matches Layers (PML) domain has dimensions of [6 cm × 6 cm] and the air domain has dimensions of [85 cm × 6 cm]. Both domains are discretized by structured quadrilateral elements with a maximum length of 0.85 cm. The MPP 1 and MPP 2 are discretized using unstructured triangular elements with a maximum length of 0.3 cm. All elements are well below $\lambda_{min}/6$, with λ_{min} is the minimum wavelength of the incoming wave. Considering that the thin parallel MPP can be used as an absorber on a room's wall, it is acceptable to assume that the MPP absorber's practical layout will be as indicated with a periodic arrangement as shown in Figure 1- Thin parallel structure of MPP: (a) 3D-coiled structure, (b) schematic of coiled parallel MPP,. In COMSOL Multiphysics 5.6, this periodicity is represented by the Floquet's periodic BC. As illustrated in Figure 2, this periodic BC is enforced at the orange line.

Additionally, the impedance BC is imposed on the thin parallel MPP surface (red line), whereas all other surfaces are defined as rigid wall (black line).

To obtain the absorption coefficient (α) of the thin parallel MPP structure, the power of the incident wave (W_{in}) and the power of the dissipated wave (W_{diss}) on the impedance BC (see Figure 2) are computed. Both powers are computed by integrating the sound intensity on the thin parallel MPP surface as:

$$\alpha = \frac{W_{diss}}{W_{inc}} = \frac{0.5 \operatorname{Re}(\mathbf{n} \cdot \int p \mathbf{u}^* dS)}{0.5 \operatorname{Re}(\mathbf{n} \cdot \int p_{inc} \mathbf{u}_{inc}^* dS)}. \quad (2)$$

p, \mathbf{u} are the total sound pressure and velocity vector at the impedance BC, respectively. The integration is over the whole surface of the MPP-1 and MPP-2. It is important to notice that the dissipated power should be positive in all frequencies, to ensure that the sound energy is absorbed into the MPP system. The MPP-1 has $D = 15.78$ [cm], and $d_2 = 8.28$ [cm], where the MPP-2 has $D_2 = 7.5$ [cm]. The $L_1 = L_2 = 3$ [cm]. Both MPP has the same properties where the diameter of the perforation hole is 0.3 [mm], and the distance between hole is 2 [mm].

3 Results and discussion

3.1 Effect of oblique incidence

To determine the effect of the incident angle on the absorption coefficient of the thin parallel MPP structure, the θ is varied from 0° to 85° with an interval of 5° , as shown in Figure 3. As seen in this figure, the absorption coefficients from 0° to 25° have two absorption peaks due to MPP 1 and MPP 2. At incidence angles greater than 30° , the two absorption coefficient peaks get closer together as a result of a better match to the air impedance, resulting in an increase in the absorption coefficient between those two peaks. When the sound enters at a greater incident angle, up to 60° , the absorption coefficient improves. However, the absorption coefficient drops when the incident angle exceeds 60 degrees. The absorption coefficient rapidly drops at high grazing incidence ($>80^\circ$). This is because the MPP's overall surface impedance is more out of phase with the air impedance. Another interesting phenomenon is the absorption of the third peak at approximately 900 Hz. At a greater angle of incidence, the peak drops to a lower frequency.

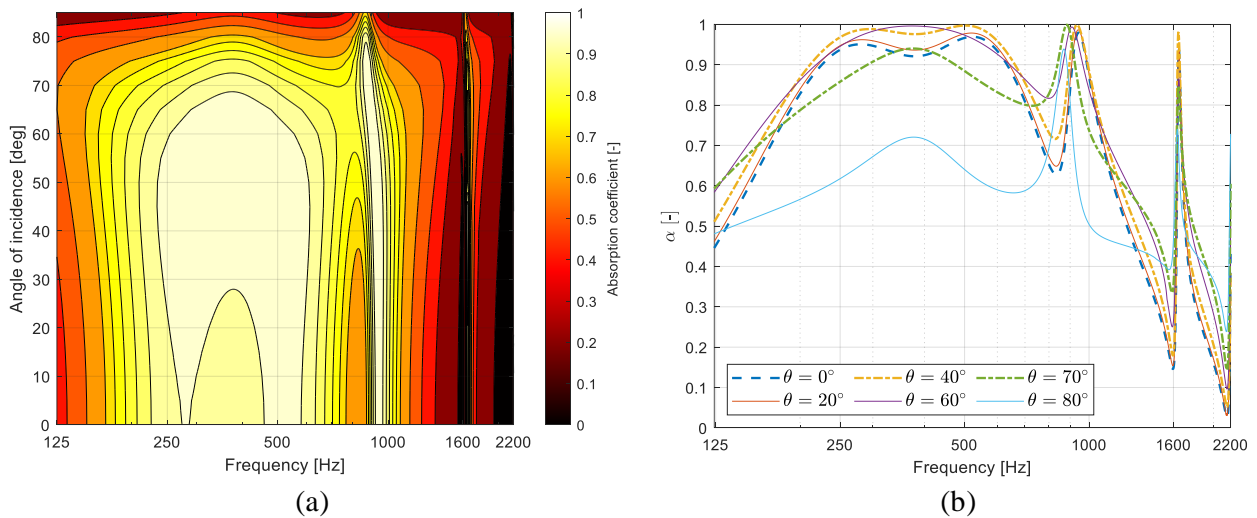


Figure 3. The absorption coefficient obtained by the FEM for the thin parallel MPP structure with (a) the variation over incident angle between 0° - 85° , and (b) the with certain incident angles.

It is critical to note that equivalent circuit analysis can be utilized to determine the sound absorption of a thin parallel MPP structure at an incidence angle θ . The absorption coefficient at various angles is calculated using Equation 1, and the results are shown in Figure 4. It is discovered that the estimation performed via equivalent circuit analysis agrees well with the numerical results.

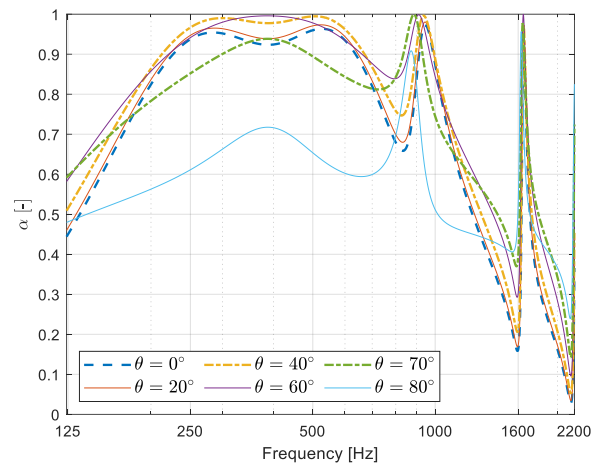
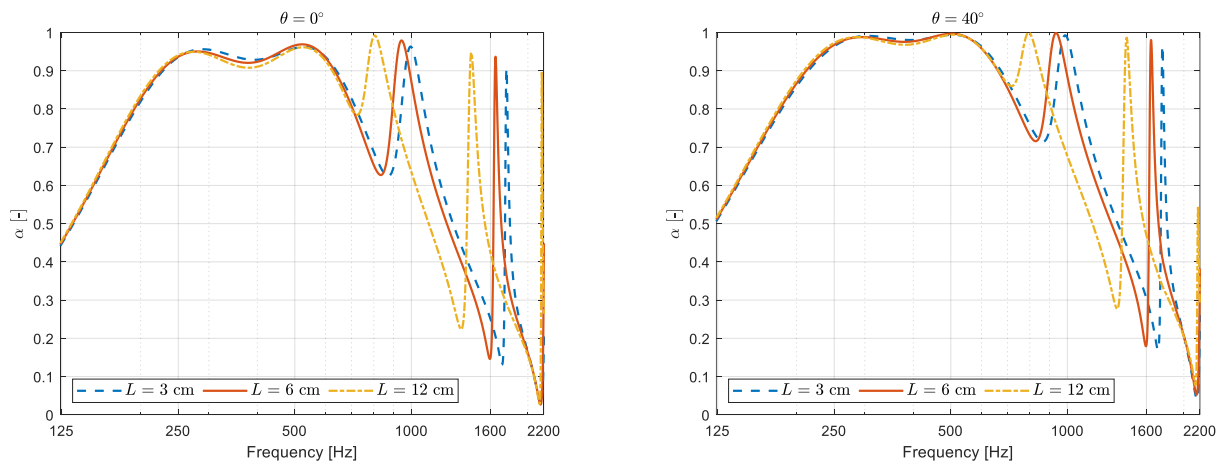


Figure 4. The absorption coefficient obtained by the equivalent circuit analysis for the thin parallel MPP structure with certain incident angles.

3.2 Effect of unit cell dimension

The current width of the unit cell, i.e. 6 cm, is adjusted by a factor of two to explore the influence of the unit cell dimension on the absorption coefficient. The results are illustrated in Figure 5, which considers incidence angles of 0° , 40° , 60° and 80° . It is obvious that the unit cell width has little effect on the absorption characteristics, with the exception of the third and fourth absorption peaks. It is discovered that a broader unit cell can result in a frequency shift of the third and fourth peaks. As a result, the breakdown frequency phenomenon is not observed in the examined situation of an oblique incidence sound wave. The breakdown frequency phenomenon implies that the sound absorption performance deviates from that of a normal incidence. Additionally, the suggested system is insensitive to oblique sound incidence up to 70° degrees, which is advantageous from a practical standpoint, as oblique incidence is generally present below 80° degrees.



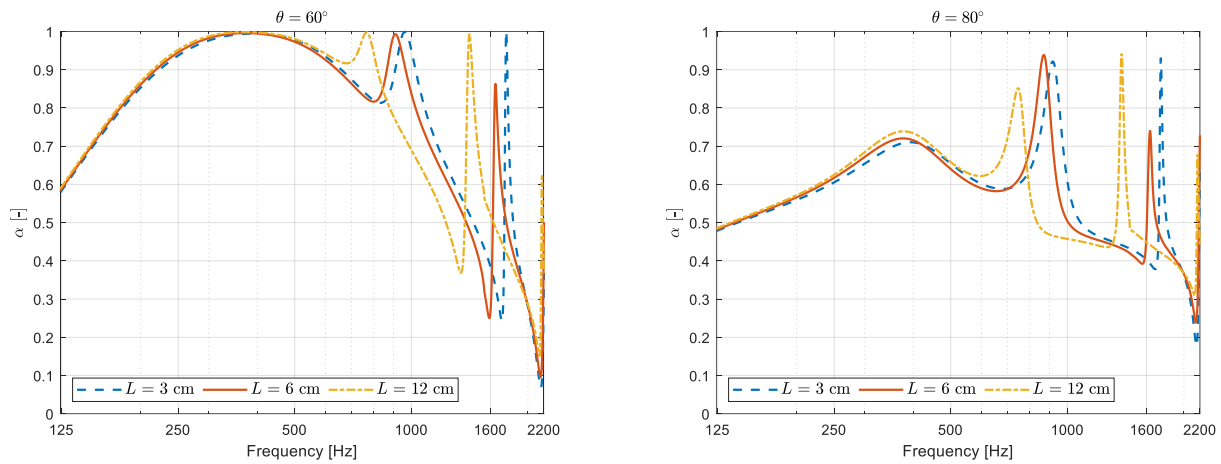


Figure 5. Effect of incidence angle on absorption characteristics for different unit cell width.

To further confirm the presence of a break down frequency, the unit cell's width is increased to 24 c m. It is obvious that the breakdown frequency of approximately 550 Hz exists for incidence angles of 60° and greater. Wang et al. [4] also discovered the breakdown frequency issue in the case of several straight cavities.

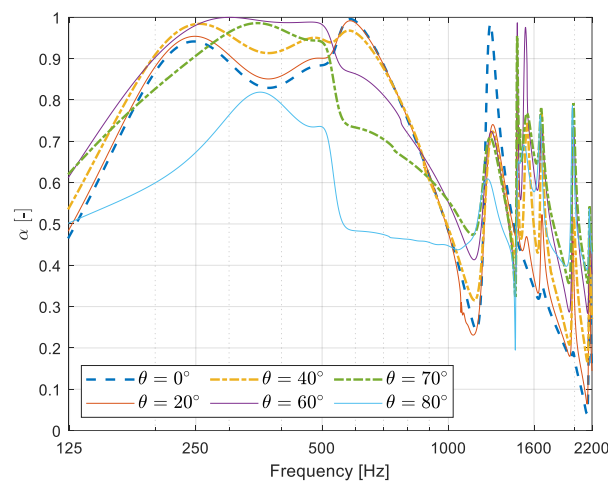


Figure 6. Width extension effect on absorption coefficients for various incidence angle.

3.3 Consequence of coiled structure

The comparison of sound absorption between a straight backing cavity and a coiled one with identical perforation characteristics is shown in Figure 7. However, the MPP with coiled backing cavity may function more robustly at higher incidence angles. As illustrated by the 70° and 80° instances, larger incidence angles result in more prominent sound absorptions near the resonance frequency. This phenomenon occurred as a result of the coiled structure's effective path length contributing to the MPP's better matching impedance. This implies that both the cavity width and the coiled orientation must be considered, as both affect the effective path length. For straight tubes, the only parameter defining the breakdown frequency at a given incidence angle is the cavity width. As a result, the design of coiled structure may be more intriguing than that of a straight tube.

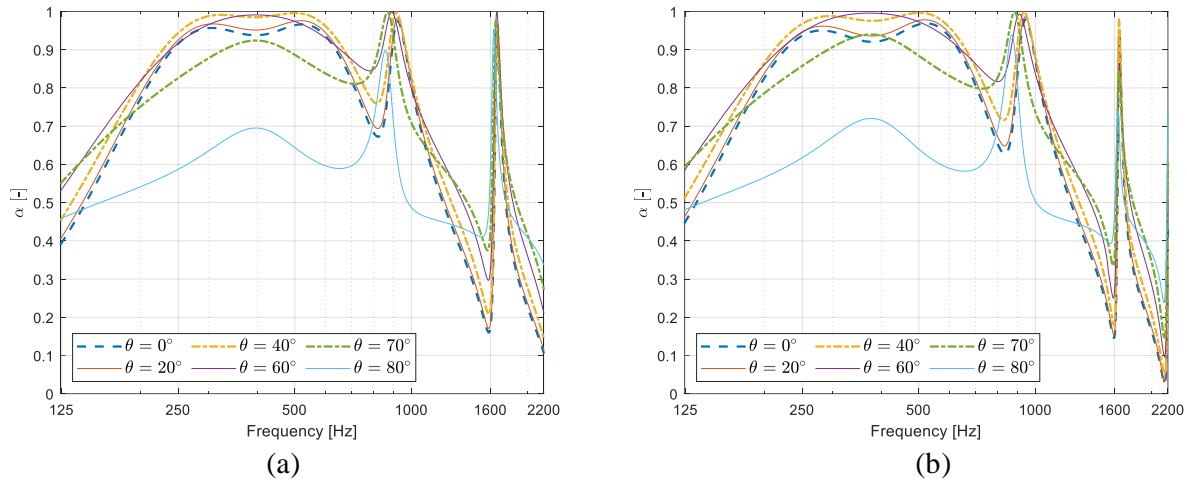


Figure 7 Absorption coefficient for the parallel MPP structure with (a) straight tube backing cavity, and (b) coiled backing cavity.

4 Conclusions

The sound absorption characteristic of a thin MPP absorber under oblique incidence has been studied. Compared with the straight backing cavity, the presence of coiled backing cavity in the thin MPP has introduced other consideration to deal with the breakdown frequency. It is found that cavity width and coiled orientation should be addressed carefully as both parameters determine effective path length and thus the acoustic reactance may be different. Moreover, smaller unit cell is preferable to avoid deterioration under oblique incidence, where the current structure can withstand the incidence angle up to 70° . Additionally, this work developed a structure for a sound absorber that is insensitive to oblique incidence, which is often present below 80° .

Acknowledgements

The authors would like to express their sincere gratitude to DIKTI/BRIN Indonesia for providing funding through the Excellent Basic Research of University Program 2021.

References

- [1]. Attenborough, K., The prediction of oblique-incidence behaviour of fibrous absorbents. *Journal of Sound and Vibration*, 1971. **14**(2): p. 183-191.
- [2]. Allard, J.F., Bourdier, R., and L'Esperance, A., Anisotropy effect in glass wool on normal impedance in oblique incidence. *Journal of Sound and Vibration*, 1987. **114**(2): p. 233-238.
- [3]. Wang, C. and Huang, L., On the acoustic properties of parallel arrangement of multiple micro-perforated panel absorbers with different cavity depths. *The Journal of the Acoustical Society of America*, 2011. **130**(1): p. 208-218.
- [4]. Wang, C., Huang, L., and Zhang, Y., Oblique incidence sound absorption of parallel arrangement of multiple micro-perforated panel absorbers in a periodic pattern. *Journal of Sound and Vibration*, 2014. **333**(25): p. 6828-6842.

- [5]. Liang, Z. and Li, J., Extreme Acoustic Metamaterial by Coiling Up Space. *Physical Review Letters*, 2012. **108**(11): p. 114301.
- [6]. Liang, Z., Feng, T., Lok, S., Liu, F., Ng, K.B., Chan, C.H., Wang, J., Han, S., Lee, S., and Li, J., Space-coiling metamaterials with double negativity and conical dispersion. *Scientific Reports*, 2013. **3**(1): p. 1614.
- [7]. Liu, Y., Xu, W., Chen, M., Yang, T., Wang, K., Huang, X., Jiang, H., and Wang, Y., Three-dimensional fractal structure with double negative and density-near-zero properties on a subwavelength scale. *Materials & Design*, 2020. **188**: p. 108470.
- [8]. Zhu, Y.-F., Zou, X.-Y., Liang, B., and Cheng, J.-C., Broadband unidirectional transmission of sound in unblocked channel. *Applied Physics Letters*, 2015. **106**(17): p. 173508.
- [9]. Al Jahdali, R. and Wu, Y., High transmission acoustic focusing by impedance-matched acoustic meta-surfaces. *Applied Physics Letters*, 2016. **108**(3): p. 031902.
- [10]. Chen, J.-S., Chen, Y.-B., Cheng, Y.-H., and Chou, L.-C., A sound absorption panel containing coiled Helmholtz resonators. *Physics Letters A*, 2020. **384**(35): p. 126887.
- [11]. Huang, S., Fang, X., Wang, X., Assouar, B., Cheng, Q., and Li, Y., Acoustic perfect absorbers via Helmholtz resonators with embedded apertures. *The Journal of the Acoustical Society of America*, 2019. **145**(1): p. 254-262.
- [12]. Almeida, G.d.N., Vergara, E.F., Barbosa, L.R., and Brum, R., Low-frequency sound absorption of a metamaterial with symmetrical-coiled-up spaces. *Applied Acoustics*, 2021. **172**: p. 107593.
- [13]. Prasetyo, I., Sihar, I., and Sudarsono, A.S., Realization of a thin and broadband Microperforated panel (MPP) sound absorber. *Applied Acoustics*, 2021. **183**: p. 108295.
- [14]. Li, D., Huang, S., Mo, F., Wang, X., and Li, Y., Low-frequency broadband sound absorber based on composite structure of micro-perforated plate and coiled back cavity. *Chinese Science Bulletin*, 2020. **65**(15): p. 1420-1427.
- [15]. Liu, C.R., Wu, H.J., Yang, Z., and Ma, F., Ultra-broadband acoustic absorption of a thin microperforated panel metamaterial with multi-order resonance. *Composite Structures*, 2020. **246**: p. 112366.
- [16]. Maa, D.-Y., Potential of microperforated panel absorber. *The Journal of the Acoustical Society of America*, 1998. **104**(5): p. 2861-2866.